Testing and Analysis of PICOSEC MicroMegas Precise Timing Detectors

Michaela Robert

Queen's University, Kingston, Ontario, Canada

E-mail: michaela.robert@queensu.ca

Abstract: Today's high energy physics experiments require precise timing detectors to enable accurate track reconstruction and identification of vertices from which particles originated. The PICOSEC collaboration is developing a MicroMegas based detector aimed at achieving high precision timing performance, currently showing results in the range of tens of picoseconds. The GDD team at CERN has designed and built multiple prototypes of the PICOSEC detector with goals of achieving large scalability, optimizing timing resolution and improving robustness. These prototypes, including a single channel detector and a 100 channel resistive detector, were tested and analyzed during the July 2022 test beam campaign which utilized CERN's Super Proton Synchrotron H4 beam line as a muon beam source. This work outlines the methodology of stability and operation testing completed on the 100 channel resistive PICOSEC prototype in preparation for the test beam. The detector showed stability to anode and cathode voltages of 711 V and -809 V, respectively, and proper response to a photon source. It also describes the single photoelectron and muon beam measurements taken at the test beam with a single channel PICOSEC prototype, and post test beam analysis for studies of the number of photoelectrons generated at the photocathode. The electron peak amplitude spectrums from single photoelectron runs were Polya distributed. The Polya fits on the spectrums from muon beams showed poor goodness of fit due to events occurring outside of a 2 mm radius of the detector's center, where the full 6 mm diameter Cherenkov cone is not incident on the photocathode. Tracking data from the test beam telescope's GEM tracking system should be used to veto events outside the center region of the detector for future analysis.

Supervised by: Marta Lisowska, Antonija Utrobicic

Contents

1 Introduction **1**
1.1 PICOSEC Detector Concept 2
1.2 Timing Resolution 3
1.3 PICOSEC Prototypes 4
1.3.1 Single Channel PICOSEC 4
1.3.2 100 Channel Resistive PICOSEC 4

2 100 Channel Resistive Prototype Stability and Operation Testing **5**
2.1 Setup 6
2.2 Stability Testing 6
2.3 Operation Testing 7

3 Photoelectron Measurements **7**
3.1 Photocathodes 8
3.2 Test Beam Setup 9
3.3 Measurements 10
3.4 Single Photoelectron Analysis 10
3.5 Polya Fitting 12
3.5.1 LED Run Results 13
3.5.2 Muon Beam Run Results 14
3.6 Spacial Event Vetoing 14

4 Conclusion **15**

5 Appendix **17**

1 Introduction

Energies and collision rates in High Energy Physics (HEP) are increasingly large, scaling with advances in accelerator and superconductor technologies. Experiments studying particles in such environments require detectors that are capable of reading out signals with high timing resolution, for example, in order to perform accurate track reconstruction to identify the vertices from which particles originated, and minimize overlapping of signals from fast consecutive events [1]. The PICOSEC MicroMegas (MM) collaboration aims to develop a spatially scalable, stable and robust gaseous detector with timing resolution in the range of tens of picoseconds. CEA Saclay and the Gaseous Detector Development (GDD) team at CERN have developed some prototypes of the PICOSEC MM detector, which are being tested and studied to further optimize timing resolution, detector stability and robustness.

A 100 channel PICOSEC detector has undergone testing at previous test beam campaigns, however a new 100 channel prototype that uses a resistive MM has never been tested. The first objective of this work was to show that the resistive prototype and its housing would be electrically stable to a margin of 1.5 times its operating voltages. Measurements of the photoelectron conversion efficiencies of various photocathodes have also been done previously, but the results are thought to have been biased by pressure changes in the unsealed detector housing between measurements. A second objective of this work was to obtain similar measurements from a single channel PICOSEC inside a vacuum chamber housing, and improve analysis methods for the calculation of the number of primary charges being generated.

1.1 PICOSEC Detector Concept

A PICOSEC MM detector consists of a MM amplifying structure, a Cherenkov radiator and a photocathode, as illustrated in Figure 1. The Cherenkov radiator is typically a MgF_2 crystal, with a photocathode material evaporated onto one of its surfaces. Various photocathode materials and thicknesses are being tested in PICOSEC detectors, as discussed further in Section 3.1, with the baseline being a semi-transparent 18 nm thick CsI photocathode. An incoming charged particle interacts inside the crystal, causing an emission of UV photons which propagate in a Cherenkov cone toward the photocathode. Photons are converted to photoelectrons in the photocathode via the photoelectric effect, and this phenomenon occurs with a quantum efficiency that is a function of the photon energy and the photocathode material, thickness and voltage. The region between the photocathode and the MM structure is called the drift gap or pre-amplification gap. The width of the drift gap is defined by the thickness of the spacer, which varies between 180 and 220 um for the current prototypes. The photocathode is biased at a negative high voltage, usually between -450 V and -500 V, while the mesh is grounded. The detector is filled with an operating gas mixture of $Ne:C_2H_4:CF_4$ in a ratio of 80:10:10. The gas has been optimized by the COMPASS collaboration to for high electron gain through avalanching, and good stability. Neon is easily ionized, C_2H_4 provides stability by absorbing UV photons, and CF_4 provides stability through attachment, and enables a fast drift velocity [2]. Primary electrons originating at the photocathode are drifted toward the mesh by the electric field in the pre-amplification region, and avalanche in the gas. The standard mesh is composed of wires which are 18 μm in diameter and has a 51% electron transparency, capturing some free electrons as they drift through [2]. The region between the mesh and the anode, called the amplification gap, is defined by the height of the bottom coverlay and the pillars and is chosen to be 128 um thick. The anode is biased at a positive high voltage, usually between +250 V and +300 V, to continue to avalanche and drift electrons toward the anode.

A typical PICOSEC readout signal induced by a single event is presented in Figure 2. As charges drift in the amplification region, their electromagnetic fields induce a current in the anode. Electrons drift quickly toward the anode, inducing a short, large amplitude 'electron peak' current signal in the anode. Ions produced during avalanching drift more slowly toward the mesh, inducing a longer and lower amplitude 'ion tail' that continues in time after the electron peak. The small currents induced in the anode are amplified by an external preamplifier, before being measured by the oscilloscope.

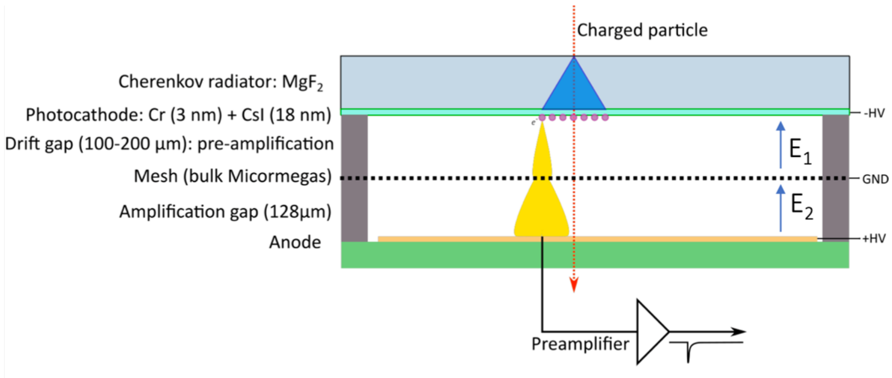

Figure 1. General schematic of PICOSEC MM detectors. Alternate photocathodes with differing materials and thicknesses may be inserted into the detector for various studies [3].

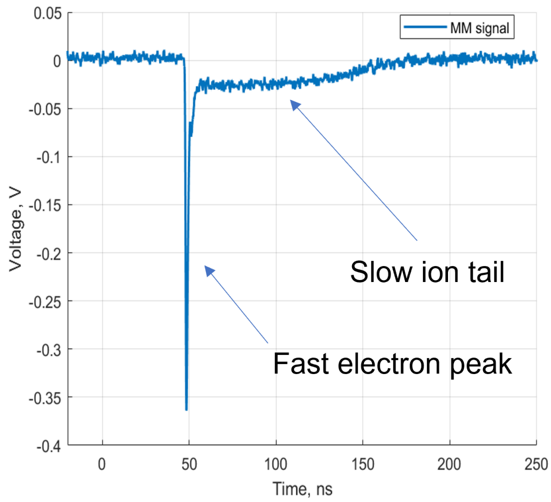

Figure 2. Sample readout voltage signal produced by a PICOSEC detector [4].

1.2 Timing Resolution

Timing resolution describes the temporal precision of a measurement of the time a particle passed through a detector. This metric is dependent on many detector settings, including the gas mixture, gas density, the field magnitudes and widths of the preamplification and amplification regions, and thickness and material of the photocathode. The effect of the thickness and material of the photocathode on timing will be further discussed in Section 3. Figure 3 shows preliminary timing data taken with a single channel PICOSEC prototype during the July 2022 testbeam campaign. A histogram is generated where each entry corresponds to the signal arrival time for one event. The time, with respect to another precise timing reference detector, when the amplitude of the readout signal has risen to 20% of the maximum amplitude of the electron peak for the current event is defined as the signal arrival time [5]. The final timing resolution metric is the standard deviation of the signal arrival time distribution.

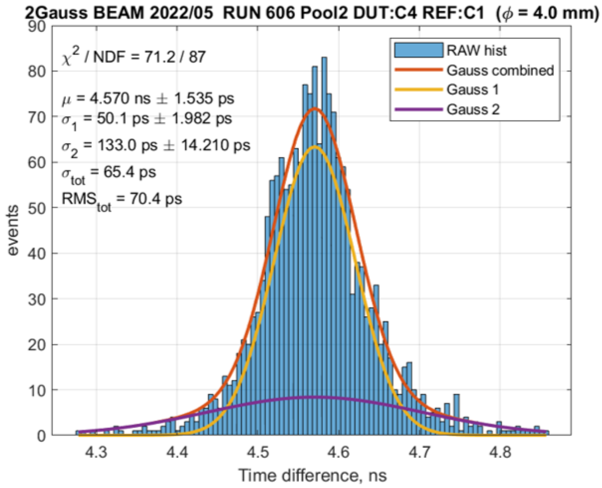

Figure 3. Histogram of signal arrival times for July testbeam run 606 using the single channel vacuum chamber prototype, MM2. The histogram is fitted with Gaussians for timing resolution analysis. Data is preliminary.

1.3 PICOSEC Prototypes

Throughout the development of PICOSEC detectors, multiple detector prototypes have been designed and tested. Two prototypes are relevant for the presented work; a single channel PICOSEC enclosed in a vacuum chamber housing, and a 100 channel resistive multipad PICOSEC.

1.3.1 Single Channel PICOSEC

The single channel PICOSEC used for the single photoelectron analysis described in Section 3 is pictured in Figure 4. The MgF_2 crystal with a photocathode evaporated on one side was changed numerous times to test different photocathode configurations. The 180 μm thick copper spacer is connected to the cathode HV input wire on the left side of the image. The MM amplifying structure, seen in the Figure as the green PCB, consists of a woven mesh of 18 μm thick steel wires and six 128 μm high pillars placed hexagonally around the center. The copper anode on the MM PCB below the mesh is not visible. The PCB contains ground and anode connections to the MM at the top of the image. The operation of the detector is as described in Section 1.1.

1.3.2 100 Channel Resistive PICOSEC

The new 100 channel resistive PICOSEC is pictured disassembled in Figure 5. A MgF_2 crystal with a photocathode evaporated on one side, similar to the cathode inside the housing in Figure 5(a), is placed over a 180 μm spacer on top of the 100 pad MM board pictured in Figure 5(b). The standard 18 μm diameter mesh is connected through 0 Ω resistors on the edges of the board to ground, and the amplification gap between the mesh and the anode is set by a 128 μm pillars in the corners and centers of the pads. The output signal from each pad is read through an isolated readout anode and contact on the back side to the outer board pictured in Figure 5(c). The resistive PICOSEC operates similarly to the non-resistive detector described in Section 1.1, with differences in the anode and readout. In a resistive PICOSEC detector, the copper anode is replaced with an

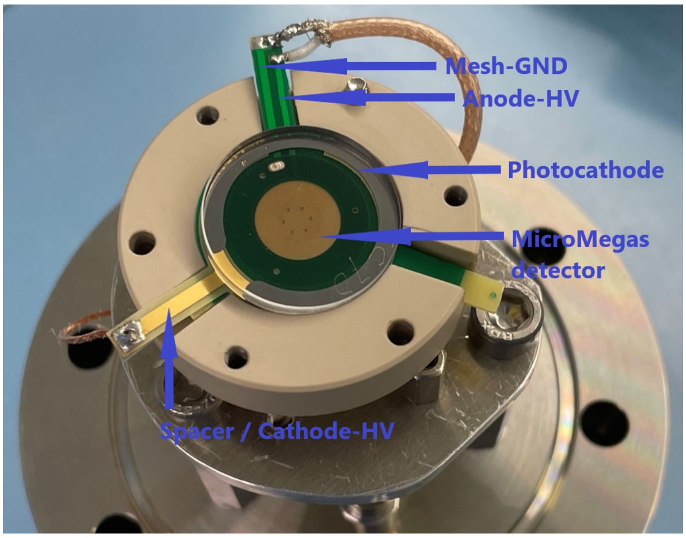

Figure 4. Single channel PICOSEC with a MgF_2 crystal, 7 nm B_4C photocathode, 180 μm pre-amplification spacer, 18 μm mesh and 128 μm pillars, attached to the front flange of the vacuum chamber housing.

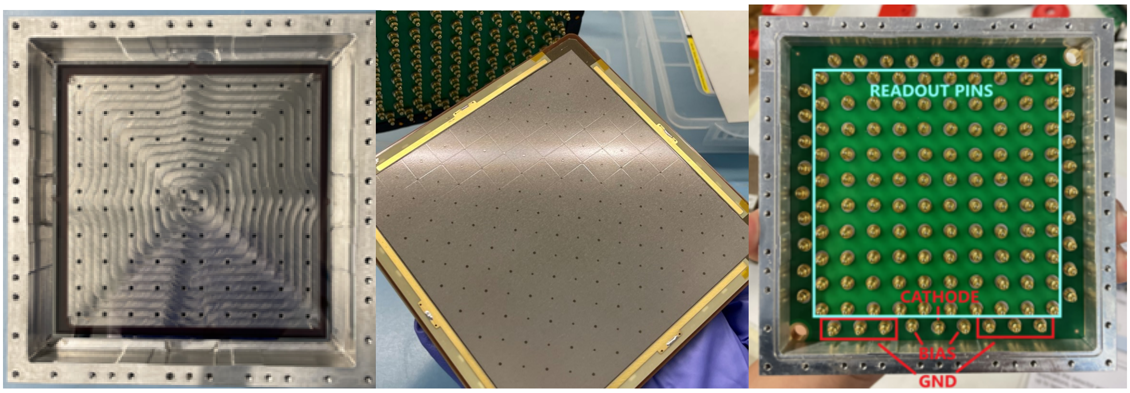

(a) Cathode (b) Resistive MM board (c) Outer board

Figure 5. Components of the 100 channel resistive PICOSEC.

anode of a 20 M$\Omega/\square$ resistive material, and an insulating layer and a separate readout pad are placed below the resistive anode. In this configuration, currents are induced in the readout pad by both the electromagnetic fields of moving charges in the amplification region, and the resistive anode. The main advantage of introducing a resistive anode is the improvement of the detector's stability at high voltages, by reducing the current in the anode caused by discharges when they occur [5]. This enables stable operation in intense pion beams, where a non-resistive detector would be unstable.

2 100 Channel Resistive Prototype Stability and Operation Testing

The newly designed and manufactured 100 channel resistive detector is expected to operate in a stable state at high voltages in order to achieve precise timing results. However, there are many components on the outer board, pictured in Figure 5(c), between which large potentials or electric fields exist, and sparking can occur. In the event of a spark, a large current is seen in the readout anode. Such sparks can damage detector components, and disrupt the operation of the detector for a period of time that extends after the sparking has quenched and the detector restabilized. Prior to the July 2022 testbeam campaign, the outer board of the 100 channel resisitive PICOSEC prototype was tested for electrical stability at high voltages, and the 100 channel PICOSEC was tested for proper response to a photon source.

2.1 Setup

The disassembly and reassembly of the 100 channel detector was done inside the clean room at the GDD lab. Inside the clean room, the outer board was cleaned in an ultrasonic ethanol bath and dried with nitrogen gas in effort to loosen and remove any dust particles stuck in the board which may cause sparking. The kapton frame that sits between the crystal and the outer housing was also cleaned with nitrogen. With all components clean, the detector was ready for assembly. A high voltage setup consisting of a 2 fold HV power supply, ORTEC 142PC preamplifier, and HV cable and adaptors was tested for sparking. The preamplifier was connected to a Teledyne Lecroy Waverunner 8104 1 GHz oscilloscope, so that sparking could be seen as a voltage pulse at the output of the preamplifier. An example of a waveform produced by a spark is shown in Figure 6. Sparking could also be indentified by an output current in the HV power source greater than 3 nA. The HV testing setup was confirmed to be stable up to 1000 V, and ready for high voltage stability testing of the multipad outer board.

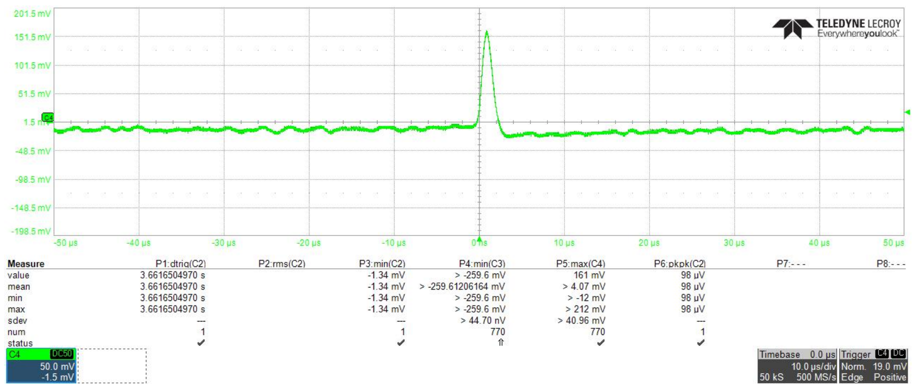

Figure 6. Signal in oscilloscope from spark event in 100 ch PICOSEC detector and amplifier.

2.2 Stability Testing

The 100 channel multipad was required to operate with a cathode voltage up to -600 V and an anode voltage up to 350 V durring the planned testing. The detector must be stable with a margin of 1.5 times the operating voltages, so the voltages on the cathode and anode were brought higher than the operating voltages during stability testing. The resistive anode, labelled Bias on the outer board and in Figure 5(c), was first placed at high voltage. To increase the potential between the Bias and adjacent readout pins, the adjacent readout pins on 2 of the 4 edges of the board were grounded by connecting the pins to the grounded outer shields, as pictured in Figure 7. Similarly, the cathode was also grounded. The anode voltage was ramped up, while periodically checking for signals of sparking on the oscilloscope and the HV power source. The threshold of instability was reached above 711 V. The procedure was repeated with the pins on the other 2 of the 4 board edges grounded, and the board showed similar stability, reaching its threshold above 711 V. The same procedure was completed with high voltage applied to the cathode, and the anode and readout pins grounded with caps. The board was deemed stable with a cathode voltage below -809 V.

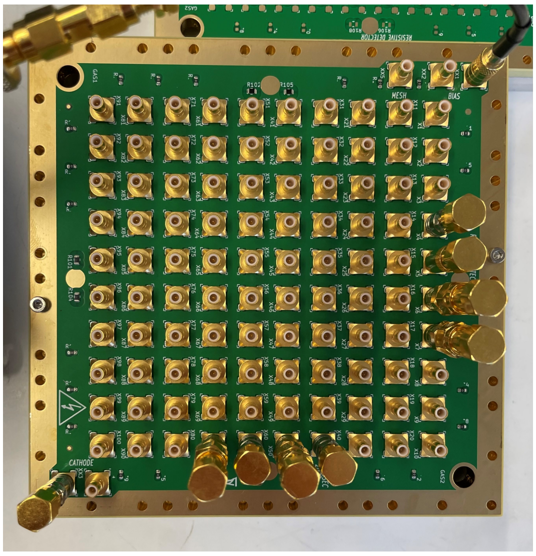

Figure 7. 100 channel PICOSEC outer board with the anode pin connected to high voltage, and the cathode pin and adjacent readouts pins on 2 of 4 board edges grounded for stability testing.

2.3 Operation Testing

After being tested for stability in air, analogical stability testing was performed with the 100 channel detector filled with the COMPASS gas mixture. The detector was first pumped 5 times, where during each pumping cycle, the inside of the housing was vacuumed to less than 1 mbar, then filled with gas. This cycle was to remove all air inside the detector before flushing it with gas during operation testing. A Cividec preamplifier was connected to the anode of pad 18 on the detector, and a UV LED was placed facing through a hole in the housing behind pad 18 to induce photoelectron emissions. The Cividec was connected to the oscilloscope and turned on, and noise with a 10 mV amplitude was visible on the oscilloscope, indicating proper operation of the Cividec. The LED was turned on, and the anode and cathode of the detector were ramped up to their operating voltages. Clear electron peak signals, such as the one displayed in Figure 8, were seen on the oscilloscope. Testing was repeated for multiple pads across the 100 channel with good response, and the detector was confirmed ready to be tested for timing resolution and other studies at the test beam.

3 Photoelectron Measurements

The timing resolution of PICOSEC MM detectors is dependent on the number of photoelectrons generated in the photocathode [2]. The physical reason for this effect is under discussion in the collaboration, but a possible explanation is to consider that the diffusion rate of a large number of

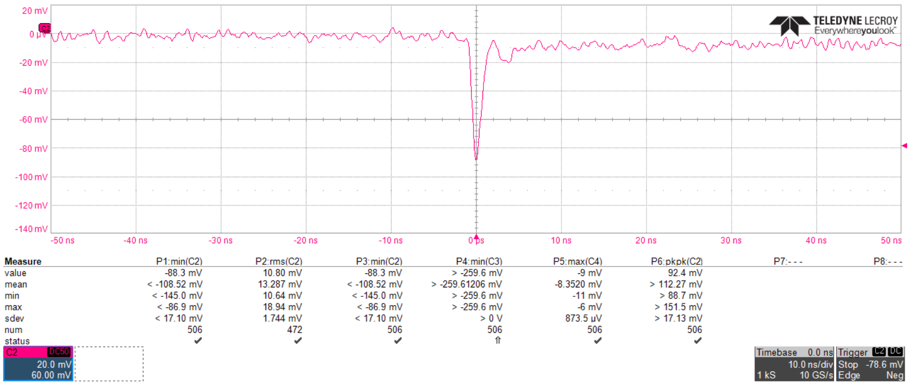

Figure 8. Signal in oscilloscope produced by 100 channel resistive board with a single photoelectron LED source. An electron peak is clearly visible and a low amplitude ion tail can also be seen, indicating good detector operation.

electrons in the direction of drifting is Gaussian distributed about some mean. In an event where 1 single primary photoelectron is generated, the photoelectron may diffuse at a rate significantly above or below the mean, causing the first avalanche to occur at a location significantly closer to or further from the mesh than the one corresponding to the mean diffusion rate. This shifts the time when the avalanche enters the amplification region, resulting in a SAT above or below the SAT for a primary electron experiencing the mean diffusion rate. When multiple primary electrons are generated at the photocathode, their diffusion rates are likely to be distributed about the expected mean for a large number of electrons, causing the average mean free path to also tend closer to that mean. The average time of charges entering the amplification region is then closer to the mean, and since the SAT is taken as the time difference when the readout current is at 20% of the electron peak amplitude, the SAT is closer to the mean. The spread and standard deviation of the SAT curve is then smaller, and the timing resolution is improved. Experimental results have shown that timing resolution is inversely proportional to the root of the number of photoelectrons, as shown in Equation 3.1,

$$\sigma(U_a, U_d, N_{p.e.}) \approx \frac{\sigma_0(U_a, U_d)}{\sqrt{N_{p.e.}}} \tag{3.1}$$

where $\sigma_0(U_a, U_d)$ is the timing resolution with single photoelectrons, and $N_{p.e.}$ is the number of photoelectrons generated at the photocathode [5].

3.1 Photocathodes

The PICOSEC group is interested in studying the efficiencies of various photocathodes and detector settings at generating photoelectrons, in order to optimize timing resolution. CsI is currently the leading photocathode material for timing resolution measurements in PICOSEC with the highest quantum efficiency, yielding approximately 10 photoelectrons per minimum ionizing particle. However, it is not an ideal material for use in large scale detectors as it can be damaged by ion feedback, humidity, sparking, and UV photons [4]. Figure 9 shows a CsI photocathode that has been severely damaged, and the white film visible on the photocathode most likely developed due to exposure to humidity after being left in air. More robust materials, including diamond-like carbon (DLC) and boron carbide (B_4C), are being studied for their photoelectron generation efficiencies, and in turn, their ability to yield good timing resolution. Experimental measurements on the photoelectron generation efficiency of various photocathodes and detector configurations are made at testbeam campaigns.

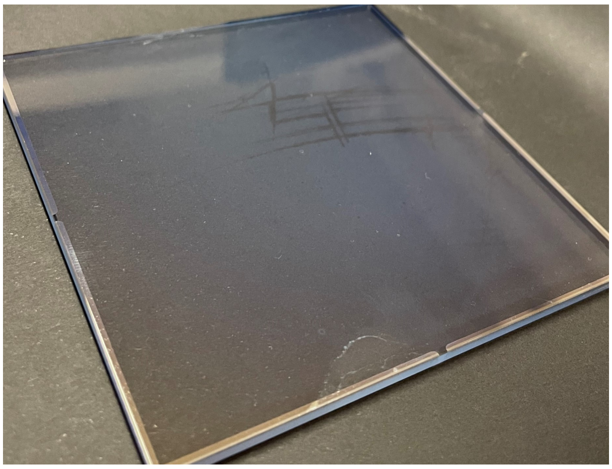

Figure 9. Damaged CsI photocathode removed from the multichannel detector after being used in the May 2022 testbeam campaign. The white film is most likely caused by exposure of CsI to humidity after being removed from the detector.

3.2 Test Beam Setup

The GDD group periodically makes use of the H4 beam line on CERN's Super Proton Synchrotron (SPS) as a particle source for testing PICOSEC and other detectors. One test beam campaign occurred in July 2022, during which the detector telescope shown in Figure 10 was tested with an 80 GeV/c muon beam source [4].

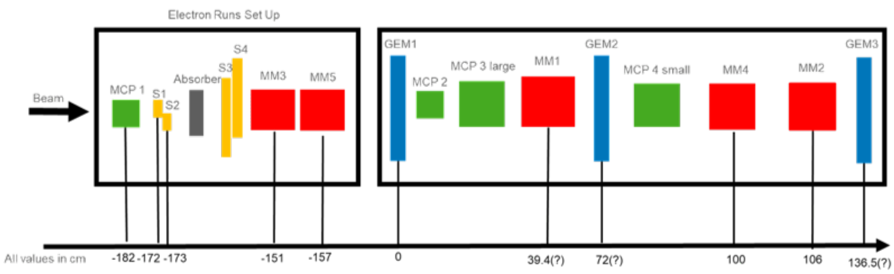

Figure 10. Schematic of the PICOSEC telescope used by the CERN GDD group in the July 2022 testbeam campaign.

The telescope consisted of 5 MM detectors which were under testing, MM1-5. MM2 was a single channel PICOSEC housed inside a vacuum chamber being used for testing the efficiency of various photocathodes at converting photoelectrons. A triple Gas Electron Multiplier (GEM) tracking system, labelled GEM1-3, was used to collect precise spacial information on incident particles for later reconstruction of their tracks through the MM detectors. Microchannel Plates (MCPs), labelled MCP1-2 and MCP3-4 large, are highly precise timing detectors which were used as references for measurements of the MM detectors. The MCPs, as well as scintillators, labelled S1-4, were used as triggering detectors. The output ports of all detectors were read using 5 Teledyne Lecroy Waverunner 8104 digital oscilloscopes, each with 4 input channels and 1 auxiliary output channel.

During each data taking run, one detector in the telescope was designated as the triggering detector. The connected oscilloscope was set to trigger on voltage signals generated in that detector by an event, and send a pulse through its output channel to an SRS system, which was connected back to an input channel on each of the 5 oscilloscopes. The SRS system generates an event ID on this signal, and relays the event ID to the other oscilloscopes in the form of a digital binary sequence. The oscilloscopes were triggered by the event ID from the SRS, and recorded waveforms from each input, including the waveform of the event ID. The event ID is read by further analysis code and used to match MM responses with the MCP timing data and GEM tracking data from the same event.

3.3 Measurements

Two seperate datasets are required to calculate the photoelectron generation efficiency of each photocathode configuration in a PICOSEC detector. The first is an LED run, during which the particle source is a UV LED which emits a single photon at once. The photon is converted to a photoelectron with a probability described by its quantum efficiency, the converted photoelectron is drifted and amplified by the MM structure, and the signal induced in the anode is recorded. The second dataset required is a muon beam run, during which the particle source is the 80 GeV/c muon beam from the SPS H4 beamline. As explained in Section 1.1, a muon that interacts in the Chernkov crystal radiates a spectrum of photons in a Cherenkov cone, which convert to electrons at the photocathode with quantum efficiencies depending on the detector configuration and photon energy. Photoelectrons originating at the photocathode are drifted and avalanched through the MM structure, inducing a signal in the anode which is recorded. Approximately 50,000 waveforms are recorded for both run types, and both runs are completed with identical detector configurations. The measurements are repeated for a number of configurations, between which the photocathode material, thickness, and voltage are varied. A summary of all single photoelectron runs completed in the July 2022 testbeam campaign is given in Table 1.

3.4 Single Photoelectron Analysis

The maximum amplitude of the electron peak from the PICOSEC detector is used to calculate the average number of photoelectrons generated per event. The electron peak amplitude from each waveform in a particular run is first extracted using MATLAB code, and a histogram of all of the maximum amplitudes is generated, as shown in Figure 11. The resulting curve consists of a main distribution that describes the probability of producing various electron peak voltages from an event with a particular detector configuration. Curve fitting is done on this section of the histogram, more

Table 1. Detector configurations for single photoelectrons completed during the July 2022 testbeam.

Runs	**LED**	**Muon Beam**
Particle Source	Single photoelectron LED	SPS H4 80 GeV/c muon beam
Trigger	MM2, trigger set at upper limit of noise	MCP2
Cathode Voltage [V]	500, 510, 520	
Anode Voltage [V]	275	
Mesh	18 μm diameter	
Gas	Ne:C_2H_4:CF_4 (80:10:10) at 990 mbar	
Photocathodes	B_4C (2, 4, 7, 10 nm), DLC with Cr, DLC without Cr	

detail on which is provided in Section 3.5, and the mean electron peak voltage is deduced from the fitted curve. The histogram also contains a tall peak at the lower end of the voltage spectrum which is attributed to noise signals in the detector output that peaked above the trigger threshold set on the oscilloscope. It is expected to see this peak because triggering is purposely set near the upper noise limit, so not to discard low voltage signals from real events and bias the probability distribution toward the higher voltage end.

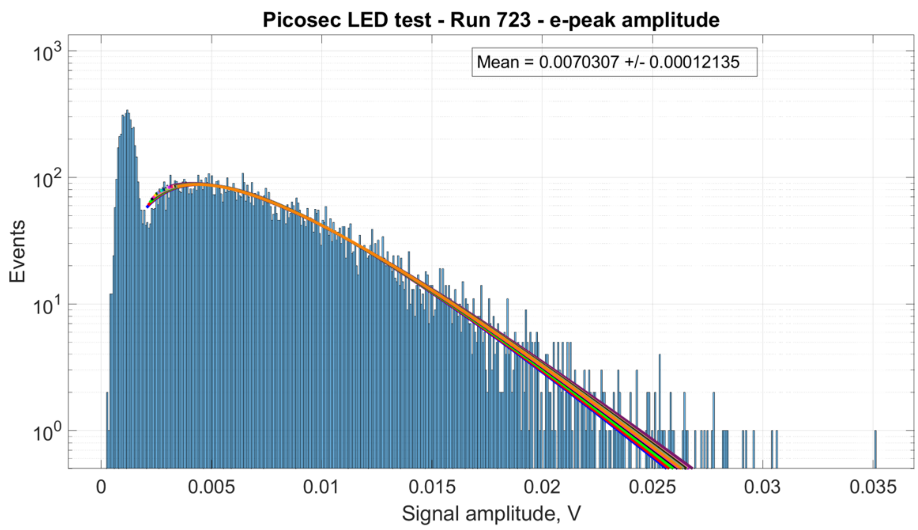

Figure 11. Hisogram of maximum electron peak amplitudes from PICOSEC MM2 LED test run 723, with a 2 nm B_4C photocathode, anode at 275 V, and cathode at 500 V. 21 Polya functions fitted to the histogram with unique lower cutoff voltages ranging from $2.0 * 10^{-3}$ V to $3.5 * 10^{-3}$ V.

The electron peak voltage extraction, histogram generation, curve fitting, and mean calculation are carried out for both the LED run, and the muon beam run of the same detector configuration. The final average number of photoelectrons, N_{pe} generated per event for a particular detector configuration is then taken as the ratio between the mean electron peak voltage from the muon beam run, $n_{\bar{n}beam}$, and the mean electron peak voltage from the LED run, $n_{\bar{n}LED}$.

$$N_{pe} = \frac{n_{\bar{n}beam}}{n_{\bar{n}LED}} \tag{3.2}$$

The N_{pe} value for various photocathodes and detector configurations are compared to learn how PICOSEC can be optimized to yield good photoelectron gain in a robust configuration, working toward a robust precise timing detector.

3.5 Polya Fitting

In pre-existing analysis code, a single negative binomial distribution was fitted to the electron peak amplitude histogram and used to calculate the mean of the curve. The lower and upper cutoff voltages were chosen visually to exclude the low voltage noise peak, as well as any high voltage saturation due to oscilloscope scaling in the histogram. As can be seen in Figure 11, the distortion of the electron peak amplitude curve due to the superposition of the low voltage noise peak degrades the goodness of fit of the negative binomial distribution, and causes uncertainty in the location of the lower end of the electron peak amplitude section of the histogram. The calculated mean of the electron peak amplitude fitted curve was shown to vary as a function of the lower cutoff voltage. This variation impacts the final average number of photoelectrons generated at the photocathode calculated from Equation 3.2. To improve the suitability of the model given non-integer voltage values, and to reduce the error introduced by uncertainty in the lower electron peak amplitude cutoff voltage, the analysis was updated to fit multiple Polya distributions with varying lower cutoff voltages to the electron peak amplitude histogram. The equation for the Polya distribution is given as [5],

$$F_i(N_i, \bar{n_i}, \theta_i, x) = \frac{N_i}{\bar{n_i}} \frac{(\theta_i + 1)^{\theta_i + 1}}{\Gamma(\theta_i + 1)} (\frac{x}{\bar{n_i}})^{\theta_i} e^{-(\theta_i+1)\frac{x}{\bar{n_i}}} \tag{3.3}$$

where,
i = index of the cutoff voltage,
N_i = normalization constant,
$\bar{n_i}$ = mean of curve,
θ_i = shape parameter

Matlab's fit function was used to fit Eqaution 3.3 to the histogram with N_i, $\bar{n_i}$ and θ_i as optimization parameters. Each Polya fitted to a given histogram took a separate voltage bin as its lower cutoff voltage. An appropriate minimum lower cutoff voltage and number of histogram bins to sweep as the lower cutoff voltage were visually determined for each histogram. The mean of each Polya was taken directly from the optimization parameter $\bar{n_i}$, and used to calculate the final mean of the electron peak curve, $n_{\bar{n}}$, as the mean of all $\bar{n_i}$ for a given histogram,

$$n_{\bar{n}} = \frac{\Sigma_{i=1}^{p} \bar{n_i}}{p} \tag{3.4}$$

where p Polyas were fitted to the electron peak amplitude histogram, equal to the number of lower cutoff voltages swept through.

3.5.1 LED Run Results

Single photoelectron LED runs exhibited peak electron amplitude spectra that were distributed very similarly to a Polya. The electron peak amplitude histogram and fitted Polyas for LED run 723 are shown in Figure 11. The variation in $\bar{n}_i$ from Polyas with various cutoff voltages is shown in Figure 12, and it may be noted that all means in the run are equal, within error. The goodness of fit for each Polya is displayed in Figure 13. All Polyas in the run have a normalized chi-square close to 1, indicating good quality fits.

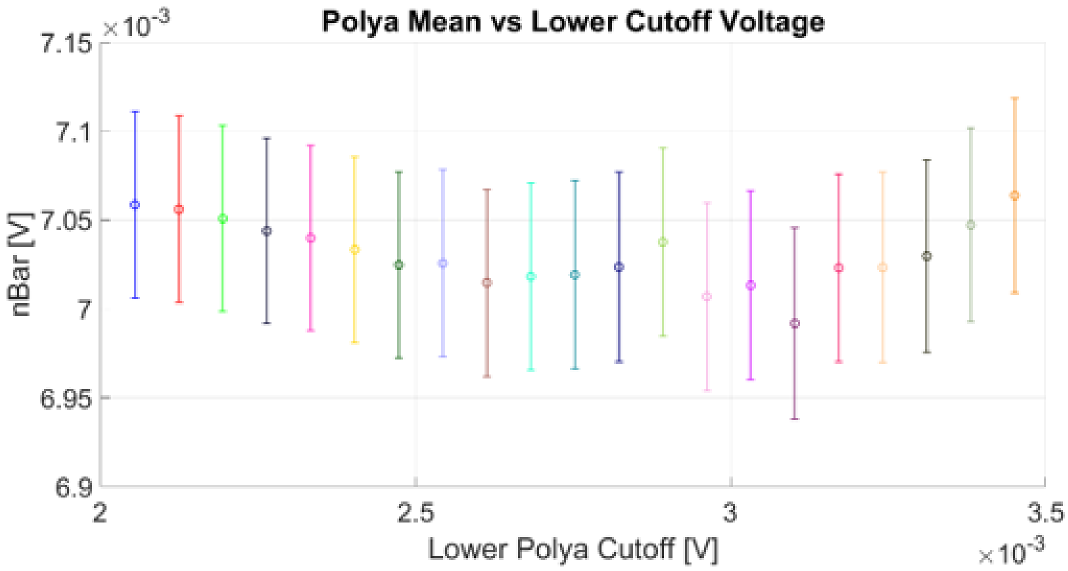

Figure 12. Mean of Polya fits using various lower cutoff voltages for PICOSEC MM2 LED run 723. Error propagation for error bars is described in Section 5.

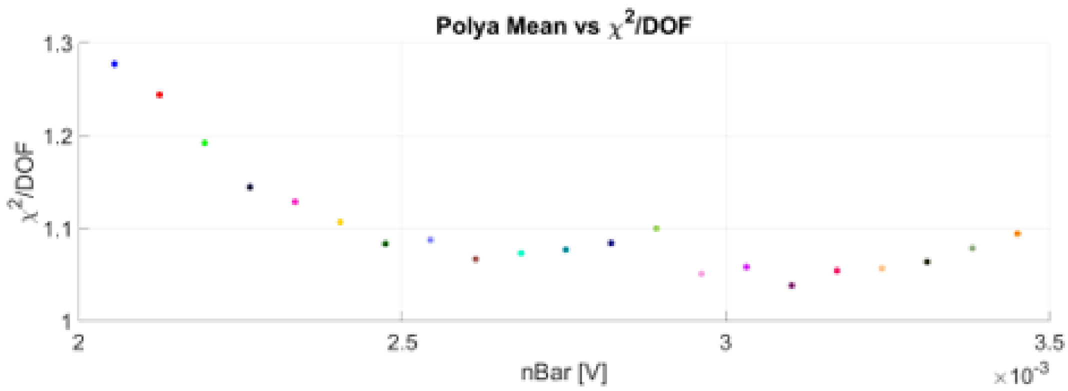

Figure 13. Normalized chi-squares of Polya fits using various lower cutoff voltages for PICOSEC MM2 LED run 723. The histogram and Polya curves for run 723 are displayed in Figure 11.

3.5.2 Muon Beam Run Results

Photoelectron muon beam runs yielded electron peak amplitude spectra that deviated significantly from Polya distributions. The electron peak amplitude histogram and fitted Polyas for muon beam run 728 are shown in Figure 14. The variation in $\bar{n}_i$ from Polyas with various cutoff voltages is larger than the error in any particular mean, as can be seen in Figure 15, indicating low confidence in the true mean of the electron peak amplitude. The goodness of fit for all Polyas are much larger than 1 as shown in Figure 16, indicating poor quality fits.

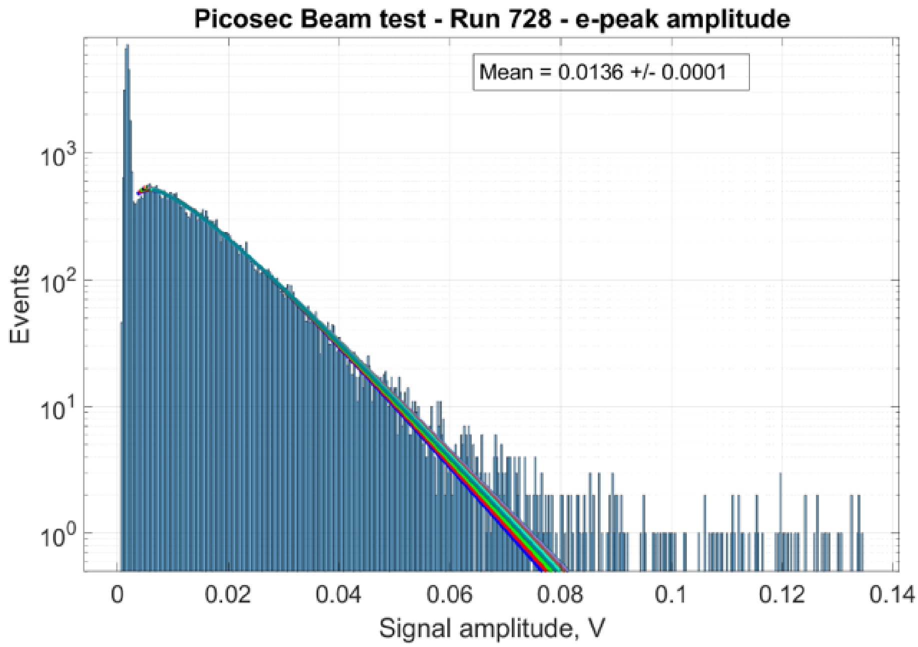

Figure 14. Hisogram of maximum electron peak amplitudes from PICOSEC MM2 muon beam test run 728, with a 2 nm B_4C photocathode, anode at 275 V, and cathode at 500 V. 11 Polya functions fitted to the histogram with unique lower cutoff voltages ranging from $3.2 * 10^{-3}$ V to $6.3 * 10^{-3}$ V.

3.6 Spacial Event Vetoing

The analysis for determining the number of photoelectrons generated at the photocathode is valid only for events which occur within a specific radius of the center of the detector, and requires additional spacial vetoing. A muon event that occurs inside the crystal produces a Cherenkov cone, which grows to approximately 3 mm in radius by the time the Cherenkov light reaches the photocathode [6]. For a PICOSEC detector that is 10 mm in diameter, the entire Cherenkov cone projects onto the photocathode only when the associated event occurs within a 2 mm radius of the center of the detector. Figure 17 illustrates this region of full enclosure with a red circle superimposed on top of a hitmap of muon events recorded by the PICOSEC and tracking system in muon beam run 728. It is evident that the cross sectional surface of the muon beam is larger than 2 mm, and many events in muon runs occurred outside of this full enclosure region of the detector.

Photons produced by events occurring outside of a 2 mm radius may be lost out of the edges of the

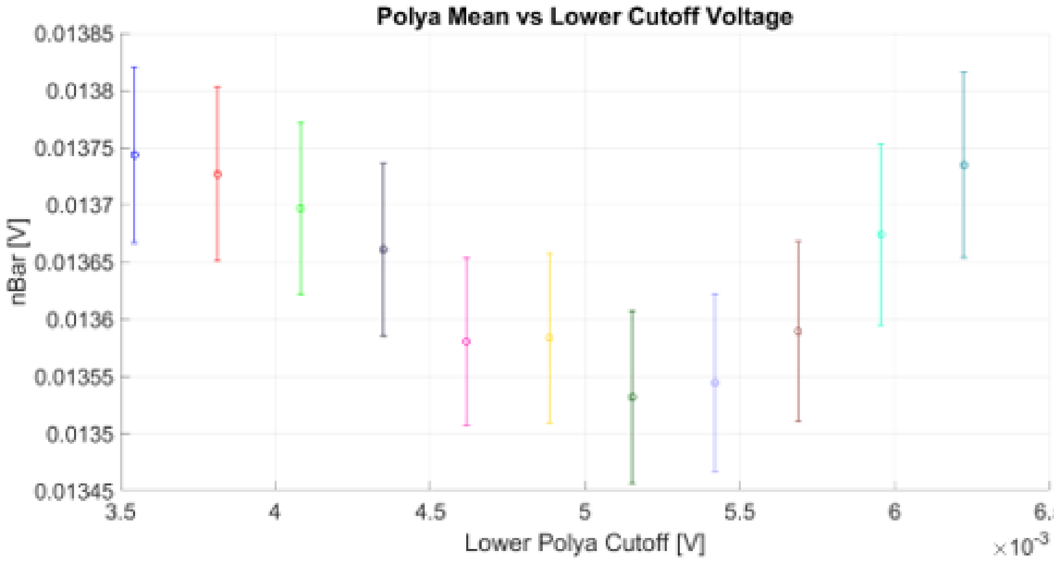

Figure 15. Mean of Polya fits using various lower cutoff voltages for PICOSEC MM2 LED run 728. Error propagation for error bars is described in Section 5.

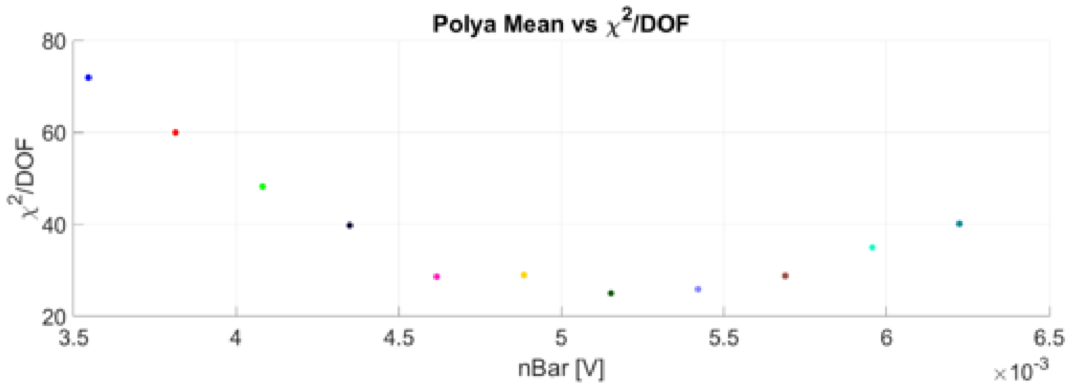

Figure 16. Normalized chi-squares of Polya fits using various lower cutoff voltages for PICOSEC MM2 LED run 728. The histogram and Polya curves for run 728 are displayed in Figure 14.

detector, and never convert to photoelectrons. The loss of primary avalanching charges results in a smaller electron peak readout voltage than an event that occurred at the center of the detector. Such events therefore pull the spectrum of electron peak voltages toward the low voltage end, creating a tail in the high voltage regime, like the one seen in Figure 14, that is not Polya-like. For future analysis, all particles hitting the detector outside of the center 2 mm radius, as reconstructed from the triple GEM tracking system, should be filtered out from the full dataset.

4 Conclusion

PICOSEC detectors are being developed as a solution for a precise timing detector that can be scaled to large experiments. Multiple PICOSEC prototypes have been developed by the GDD lab at CERN and have been put under test beam to study the impacts of various detector configurations

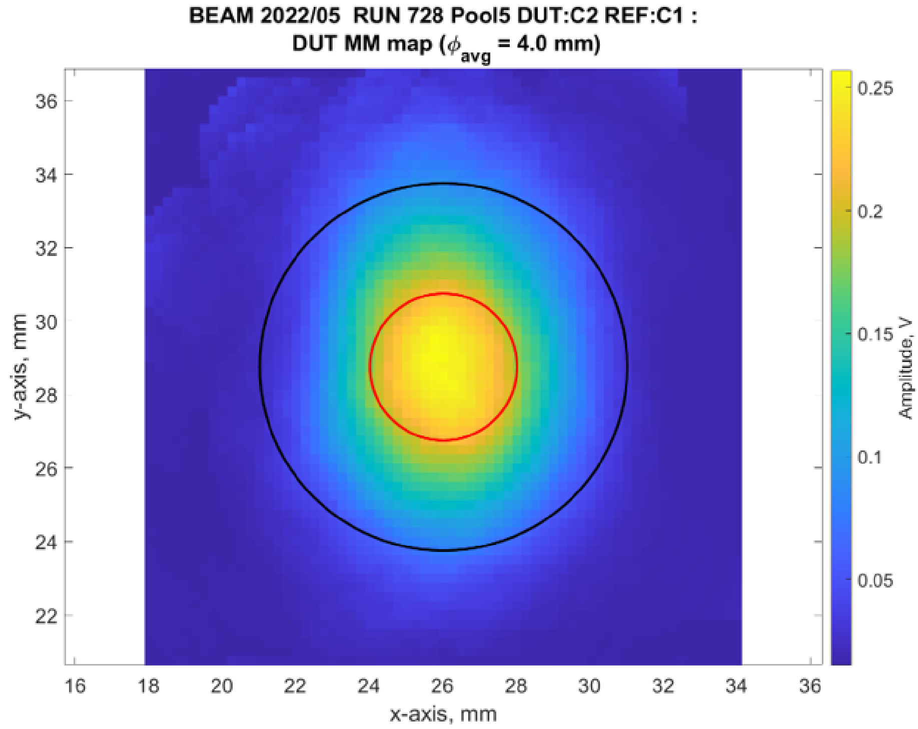

Figure 17. Hitmap of locations of events seen in PICOSEC MM2 detector during run 728, based on reconstructed tracks recorded by the PICOSEC testbeam telescope's triple GEM tracking system, shown in Figure 10. The black circle is 5 mm in radius and shows the location of the PICOSEC detector relative to events passing through. The red circle is 2 mm in radius and shows the region in which events take place with their entire Cherenkov cone projecting onto the photocathode.

on timing performance. In preparation for the July 2022 test beam campaign, the outer board of the 100 channel resistive prototype was placed under high voltage stability testing and pushed above its maximum operation point of anode/cathode 350/-600 V to show stability at anode/cathode 711/-809 V. The detector was then fully assembled and successfully tested for proper response to an LED photon source. To study the efficiency of various photocathodes and detector configurations for generating photoelectrons, a series of photoelectron datasets were taken during the test beam campaign. Existing analysis was updated to introduce a curve fitting method more suited for real-valued voltage data with the switch from negative binomial distribution to Polya fitting. A more rigorous method for calculating the electron-peak mean was implemented to help improve the accuracy of single photoelectron final results. Future improvements may be made to the analysis by implementing spacial vetoing to filter out muon events that occurred in the region of the detector where their Cherenkov cones are cut off.

I had a very enriching summer learning about gaseous detectors and gaining hands on experience with lab work and datataking. Thank you to my supervisors, Marta Lisowska and Antonija Utrobicic, as well as the GDD lab for your amazing guidance and company!

References

[1] S. White, "Experimental challenges of the european strategy for particle physics," in *Proceedings of CHEF 2013*, The Rockfeller University, 2013. https://arxiv.org/pdf/1309.7985v1.

[2] J. Bortfeldt *et al.*, "Picosec: Charged particle timing at sub-25 picosecond precision with a micromegas based detector," *Nuclear Instruments and Methods in Physics Research Section A: Accelerators, Spectrometers, Detectors and Associated Equipment*, vol. 903, pp. 317–325, 2018. https://www.sciencedirect.com/science/article/pii/S0168900218305369.

[3] A. Utrobicic, "Precise timing measurements with a 10x10cm2 tileable picosec micromegas detector module," 2022. VCI2022. https://indico.cern.ch/event/1044975/contributions/4663685/attachments/2397933/4100323/Picosec-Micromegas-VCI-A.pdf.

[4] M. Lisowska, "Sub-25 ps timing measurements with 10x10 cm2 picosec micromegas detectors," 2022. NDIP.

[5] L. Sohl, *Development of PICOSEC-Micromegas for fast timing in high rate environments*. PhD thesis, Universite Paris-Saclay, 2020. https://tel.archives-ouvertes.fr/tel-03167728/document.

[6] S. Aune *et al.*, "Timing performance of a multi-pad picosec-micromegas detector prototype," *Nuclear Instruments and Methods in Physics Research Section A: Accelerators, Spectrometers, Detectors and Associated Equipment*, vol. 993, 2021. https://www.sciencedirect.com/science/article/abs/pii/S0168900221000607.

5 Appendix

In the photoelectron analysis code, MATLAB's curve fitting function, fit(), was set to report upper and lower error on the mean $\bar{n_i}$ for a 68% confidence interval. For both the upper and lower bound, this error was propagated through the calculation of $n_{\bar{n}}$ by,

$$\Delta n_{\bar{n}} = \frac{1}{2}\left[\Sigma_{i=1}^{p}(\Delta\bar{n_i} - \bar{n_i})\right]^{\frac{1}{2}} \tag{5.1}$$

The error was then further propagated to the number of photoelectrons N_{pe} by,

$$\Delta N_{pe} = \sqrt{\left(\frac{\Delta n_{\bar{n}beam}}{n_{\bar{n}LED}n_{\bar{n}beam}}\right)^2 + \left(-\frac{n_{\bar{n}beam}}{{n_{\bar{n}LED}}^2}\Delta n_{\bar{n}LED}\right)^2}$$

(5.2)